南京航空航天大学

论文集

（二〇〇五年） 第10册

能源与动力学院

（第5分册）

南京航空航天大学科技部编

二〇〇六年三月

能源与动力学院

023 系

目录

序号	姓名	职称	单位	论文题目	刊物、会议名称	年、卷、期	类别
1	张靖周 李立国 高潮	正高 正高 副高	023 023 023	直升机排气系统红外抑制器的模型实验研究	红外与毫米波学报	2005.24.2	
2	张靖周 单勇	正高 博士	023 023	波瓣引射－混合器特性参数影响的数值研究与验证（英文）	航空学报	2005.18.3	
3	杨卫华 张靖周	中级 正高	023 023	The study of flow characteristics of curved microchannel	Applied Thermal Engineering	2005.25	
4	杨卫华 马国锋	中级 硕士	023 023	气膜冷却孔几何结构对流量系数的影响	推进技术	2005.26.5	
5	杨卫华 张靖周	中级 正高	023 023	变截面微小通道传热特性的研究	工程热物理学报	2005.26.5	
6	谭晓茗 张靖周	博士 正高	023 023	自耦合射流流动特性和相关参数影响规律的数值研究	航空动力学报	2005.20.5	
7	谭晓茗 张靖周	博士 正高	023 023	压电驱动自耦合射流冲击冷却特性的研究	航空动力学报	2005.20.6	
8	谭晓茗 张靖周	博士 正高	023 023	Heat Transfer Characteristics of a Synthetic Jet Impingement	18th National & 7th ISHMT-ASME Heat and Mass Transfer Conference	2005	
9	单勇 张靖周	博士 正高	023 023	波瓣喷管引射－混合器涡结构的数值研究	空气动力学学报	2005.23.3	
10	单勇 张靖周	博士 正高	023 023	波瓣喷管结构参数对引射混合器性能影响的数值研究	航空动力学报	2005.20.6	
11	唐正府 张靖周	博士 正高	023 023	波瓣喷管－狭长出门弯曲混合管引射混合特性分析	航空动力学报	2005.20.6	
12	李建中 王家骅 范育新 张义宁 张靖周	博士 正高 副高 博士 正高	023 023 023 023 023	煤油气动阀式脉冲爆震发动机爆震波压力特性试验	推进技术	2005.26.5	
13	李建中 王家骅 范育新 张义宁 张靖周	博士 正高 副高 博士 正高	023 023 023 023 023	煤油／空气气动阀式脉冲爆震发动机试验	航空动力学报	2005.20.5	
14	李建中 王家骅 范育新 张义宁 张靖周	博士 正高 副高 博士 正高	023 023 023 023 023	气动阀结构对爆震波压力特性影响	第十三届燃烧与传热传质专业学术讨论会论文集	2005	
15	韩启祥 王家骅	副高 正高	023 023	预混气爆震波在不同直径管间的传播特性	航空动力学报	2005.20.2	

目录

序号	姓名	职称	单位	论文题目	刊物、会议名称	年、卷、期	类别
16	唐豪 L.C. Wrobel I.E. Barton	正高 Profe- ssor lecture	023 外国 外国	Numerical experimental investigation of particle interaction in turbulent flow through a dose diffusion pipe in the detecting system	Nuclear Engineering and Design	2005.235.9	
17	唐豪 L.C. Wrobel Z.Fan	正高 Profe- ssor profe- ssor	023 外国 外国	Numerical analysis of the hydrodynamic behaviour of immiscible metallic alloys in twin-screw rheomixing process	Materials and Design	2005	
18	唐豪 L.C. Wrobel	正高 Profe- ssor	023 外国	An interface tracking method for modelling the flow of immiscible metallic liquids in rheo-mixing process	International Journal of Engineering Science	2005.43. 15-16	
19	范育新 王家骅 李建中 张义宁	副高 正高 博士 博士	023 023 023 023	脉冲爆震发动机（PDE)引射增推装置研究	航空动力学报	2005.20.6	
20	范育新 王家骅 李建中 张义宁 张靖周	副高 正高 博士 博士 正高	023 023 023 023 023	脉冲爆震发动机供油自适应控制优化设计	推进技术	2005.26.1	
21	范育新 王家骅 李建中 张义宁	副高 正高 博士 博士	023 023 023 023	脉冲爆震发动机气动阀性能分析	第十三届燃烧与传热传质专业学术讨论会论文集	2005	
22	杨敏 常海萍 房治有	博士 正高 本科	023 023 023	旋转条件下热驱动换热效果比较研究	工程热物理学报	2005.26.2	
23	杨敏 常海萍 毛军逵 白云峰	博士 正高 副高 硕士	023 023 023 023	离心力场下热驱动换热准则关系式的确定	航空动力学报	2005.20.3	
24	杨敏 常海萍 房治有	博士 正高 本科	023 023 023	模拟涡轮叶片冷却通道的热驱动实验研究	航空动力学报	2005.20.5	
25	杨敏 常海萍 夏婕 谭晓茗 毛军逵	博士 正高 博士 博士 副高	023 023 023 023 023	旋转条件下带冷却通道的热驱动换热数值分析	南京航空航天大学学报	2005.37.4	
26	夏婕 常海萍 杨敏	博士 正高 博士	023 023 023	装有多孔介质的封闭腔体中热驱动换热的数值研究	南京航空航天大学学报	2005.37.6	

目录

序号	姓名	职称	单位	论文题目	刊物、会议名称	年、卷、期	类别
27	徐磊 常海萍 雍佳昊	博士 正高 本科	023 023 023	涡轮叶片内部气膜孔局部换热特性实验研究	中国工程热物理学会第十一届学术会议	2005	
28	张净玉 常海萍	副高 正高	023 023	The Interior Heat Transfer Characteristics of Gas Turbine Blade Due to Sparse Film Cooling Holes	Heat Transfer-Asian Research	2005.34	
29	胡娅萍 吉洪湖	博士 正高	023 023	致密多孔壁冷流入射角对冷却效果影响的数值研究	航空动力学报	2005.20.1	
30	胡娅萍 吉洪湖	博士 正高	023 023	孔阵排列疏密度对致密多孔壁冷却效果的影响	推进技术	2005.26.1	
31	陈炎 吉洪湖 胡娅萍	硕士 正高 博士	023 023 023	致密微孔壁复合冷却对流换热系数研究	工程热物理学报	2005.26.3	
32	徐亮 吉洪湖	硕士 正高	023 023	旋转状态下石墨封严结构的泄漏特性数值模拟	南京工程热物理学会第八次会议	2005	
33	纪国剑 吉洪湖	博士 正高	023 023	旋转状态下篦齿蜂窝结构封严特性研究	中国工程热物理学会第十一届学术会议	2005	
34	李娜 吉洪湖	硕士 正高	023 023	涡扇发动机轴承腔冷却性能的数值分析	中国工程热物理学会第十一届学术会议	2005	
35	杨超 吉洪湖	硕士 正高	023 023	涡轮叶片竹节孔冷却通道固耦合传热的研究	中国工程热物理学会第十一届学术会议	2005	
36	刘军 吉洪湖	硕士 正高	023 023	涡轮导叶内部孔阵冲击冷却的数值模拟	中国工程热物理学会第十一届学术会议	2005	
37	王世忠 吉洪湖 胡娅萍	硕士 正高 博士	023 023 023	发动机进口支板雾淞积冰过程的数值模拟	中国工程热物理学会第十一届学术会议	2005	
38	罗明东 吉洪湖	博士 正高	023 023	有遮挡结构的无人机排气系统红外辐射特性的数值计算研究	中国工程热物理学会第十一届学术会议	2005	
39	罗明东 吉洪湖	博士 正高	023 023	国外飞行器红外辐射特性计算软件简析	隐身技术	2005.1	
40	罗明东 吉洪湖	博士 正高	023 023	高涵道比涡扇发动机排气系统红外特性的数值计算	中国航空学会第十三届燃烧与传热传质专业学术会议	2005	
41	张勃 吉洪湖	中级 正高	023 023	圆转矩形大宽高比矩形喷管射流掺混特性研究	中国工程热物理学会第十一届学术会议	2005	
42	张勃 吉洪湖	中级 正高	023 023	大宽高比矩形喷管过渡型面及喷口形状对尾喷流掺混特性的影响	中国航空学会第十三届燃烧与传热传质专业学术会议	2005	

目录

序号	姓名	职称	单位	论文题目	刊物、会议名称	年、卷、期	类别
43	陈炎 吉洪湖	硕士 正高	023 023	致密微孔壁绝热冷却效果研究	中国工程热物理学会第十一届学术会议	2005	
44	王亚彤	中级	院机关	谈大学生能否顺利就业对高校招生工作的影响	教育与职业	2005.24	
45	刘德彰	正高	院机关	目前课堂教学中若干问题的思考	南京航空航天大学学报（社会科学版）	2005.7.1	

第24卷第2期
2005年4月

红外与毫米波学报
J. Infrared Millim. Waves

Vol. 24, No. 2
April, 2005

文章编号:1001-9014(2005)02-0125-05

直升机排气系统红外抑制器的模型实验研究

张靖周, 李立国, 高 潮
(南京航空航天大学 能源与动力学院,江苏 南京 210016)

摘要:对直升机排气系统红外抑制器进行了一系列的模型试验研究,旨在分析引射混合和遮挡隔热对降低目标红外辐射特征的作用机制和抑制效果,并对缩比模型的红外辐射相似关系进行探讨.结果表明:(1)引射冷气掺混具有降低排气温度和混合管壁面温度的双重作用,其降温效果在大引射流量比下非常显著;当遮挡间距大于20mm,遮挡隔热可以使遮挡罩壁温接近于环境温度.(2)引射混合对总体红外辐射强度抑制约85%;在此基础上进行隔热遮挡可以再抑制10%.(3)在保持主流速度、温度和压力均相同的条件下,不同缩比模型的辐射亮度基本相当;红外辐射强度基本上与模型的几何模化比平方成正比.

关 键 词:红外辐射;红外抑制;引射-混合器;直升机排气系统
中图分类号:V231.3,P722.5 **文献标识码**:A

MODEL EXPERIMENTS OF INFRARED SUPPRESSOR FOR HELICOPTER EXHAUST SYSTEM

ZHANG Jing-Zhou, LI Li-Guo, GAO Chao
(College of Energy and Power, Nanjing University of Aeronautics and Astronautics, Nanjing 210016, China)

Abstract: A series of mode experiments for the infrared signature suppression (IRSS) device used in the helicopter gas turbine exhaust system were carried out to investigate the effects of ambient air pumping-mixing and heat shelter-insulation on decreasing the target infrared signature and quest for the infrared signature similarity between two scaled models with different scale factors. The results show that (1) Ambient air pumping-mixing plays a dual role for reducing the exhaust temperature and mixing duct temperature and this role is more obvious in the case of larger mass flow ratio of secondary flow to primary flow. Sheltering from the hot mixing duct wall makes the sheltering sheath temperature close to ambient temperature in case of the sheltering distance greater than 20mm. (2) Ambient air pumping-mixing contributes about 85% suppression for the total target infrared radiation intensity and heat shelter-insulation contributes about 10% suppression again. (3) While the primary flow velocity, temperature and pressure are at the same condition for different scaled models, the irradiances for different scaled models are almost the same and the infrared radiation intensity is almost proportion to the square of model scale factor.
Key words: infrared radiation; infrared signature suppression; mixer-ejector; helicopter exhaust system

引言

直升机发动机排气系统的外露壁面和燃气尾焰是红外制导武器的主要探测和攻击目标,减少红外辐射的一个有效方法是使用红外抑制器,利用排气的动量引射环境空气来实施混合降温,目前应用最为广泛的红外抑制器采用波瓣喷管-弯曲混合管结构[1~3].大量的研究表明,波瓣喷管具有诱发轴向阵列旋涡的特征,引射-混合性能优越[4~7].对于直升机而言,由于不需要通过喷气产生推力,可以利用弯曲的混合管使排气转向并遮挡发动机内部的高温部件;同时,在混合管外还可套上遮挡罩,进一步降低外露壁面的温度.

由于发动机运行的工况复杂,直接利用发动机开展红外抑制器的研究无论在成本上、还是时间上都需要付出很大代价.因此采用缩比实验模型所得到的研究结果如何推广应用于真实的状态,是红外抑制器性能分析和结构设计的一个关键问题[1~3].同时,由于红外辐射具有表面辐射和气体辐射两种来源,引射混合和隔热遮挡的红外抑制作用效果如何,目前仍未有清晰的认识.本文通过一系列的模型实验研究,对波瓣喷管-弯曲混合管引射式红外抑制

收稿日期:2004-03-01,**修回日期**:2004-09-20 **Received date**: 2004-03-01, **revised date**: 2004-09-20
基金项目:武器装备预研基金(51410040304HK0201)资助项目
作者简介:张靖周(1964-),男,江苏东海人,教授,研究方向为传热传质学与红外隐身技术.

器的气动和红外特性进行了测试，基于上述测试数据，分析了引射混合和遮挡隔热的作用机制和红外抑制效果，并对缩比模型的红外辐射相似关系进行了探讨，得出了一些有益的结论.

1 实验系统和模型

实验装置如图1所示.

主流由压气机提供，流量由标准孔板流量计测量. 经过加热器或燃烧室后从喷管流出，前者用于气动特性测试实验，后者则用于红外特征测试实验. 喷管前主流的总温和总压由安装在稳定段后部的探针测量. 环境空气依靠主流动量的引射作用驱动，通过标准入口流量管进入集气室，在混合管内与主流混合. 在标准入口流量管和集气室的联结部装有通道面积调节机构，通过改变引射气流通道堵塞比来改变引射气流流量. 两股气流混合后排入环境大气.

红外抑制器由波瓣喷管、中心锥体、弯曲混合管和遮挡罩构成(图2). 波瓣喷管的12个波瓣沿周向均布，其结构参数主要有平均直径 d_1，波瓣扩张角 α，波瓣高度 h 和宽度 b；弯曲混合管结构参数有直径 d_m，直管优长度 l，弯曲角度 β；遮挡罩结构参数是遮挡间距 s；中心锥体结构参数有入口锥角 r^2，出口锥角 φ，锥体直径 d_c. 在气动和红外特性实验中所选择的实验模型参数如表1所列.

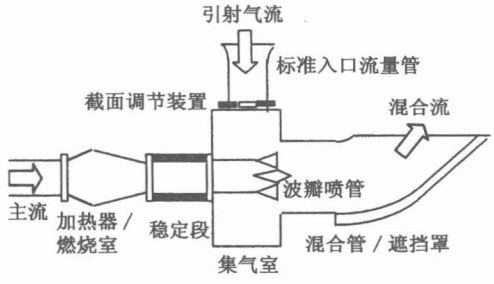

图1 实验装置示意图
Fig. 1 Schematic of experiment equipment

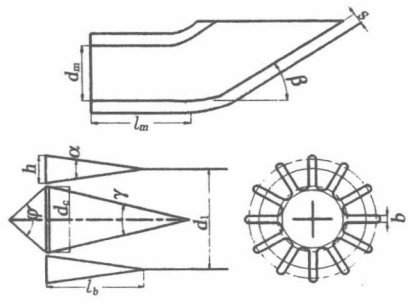

图2 实验模型示意图
Fig. 2 Schematic experiment model

表1 实验模型参数
Table 1 Structural parameters of experimental models

实验类别		气动	红外	
实验模型		小模型	大模型	小模型
喷管	d_1(mm)	45	150	75
	α(°)	25	35	35
	h(mm)	13.5	50	25
	b(mm)	5	15	7.5
中心锥	γ(°)	30	30	30
	φ(°)	60	60	60
	d_c(mm)	30	100	50
	d_m(mm)	100	300	150
遮挡罩 混合管	l(mm)	100	170	85
	β(°)	25	35	35
	s(mm)	0~35	0/30	/

2 引射流量与遮挡间距的影响

在电加热风洞上，通过改变引射气流通道的堵塞比和遮挡罩的遮挡间距，研究引射流量比和遮挡间距对混合管出口气流总温、混合管和遮挡罩底部壁面温度分布的影响. 实验条件：主流流量为0.06kg/s，总温240℃，总压102 325Pa，环境温度28℃.

图3为引射流量比($\Phi = m_p/m_s$)与引射气流通道面积堵塞比之间的变化曲线.

可以看出，引射流量比随着引射气流通道面积堵塞比的增加而下降的关系并不是线性的，在较大的堵塞比下衰减得更剧烈.

图4反映了在不同引射流量比和遮挡间距下，混合管出口气流最高温度、混合管和遮挡罩壁面最高温度的变化趋势. 随着引射流量比的增加，混合气流最高温度和混合管壁面最高温度大幅下降，且两者之间的差值也呈逐渐扩大. 表明引射冷气的作用机制是双重的，即引射气流对热气流的掺混作用和

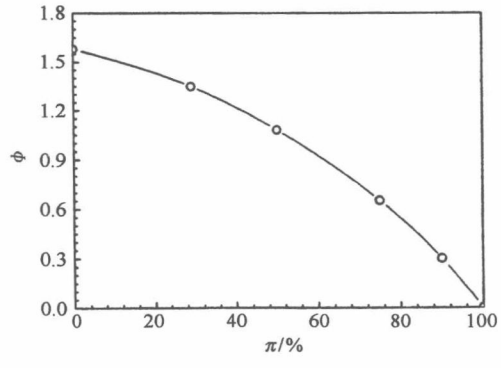

图3 引射流量比与堵塞比的关系
Fig. 3 Mass flow ratio vs block area ratio

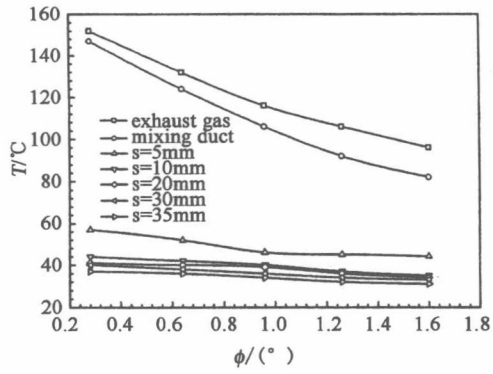

图 4　引射流量比和遮挡间距对排气和壁面温度的影响
Fig. 4　Effects of m_s/m_p and s on exhaust gas and wall temperatures

对混合管壁面的隔热防护作用. 随着遮挡间距的增加,遮挡罩壁面的最高温度在 $s=0\sim10$mm 的范围内急剧下降;在 $s=30$mm 之后,再增加遮挡间距对降低遮挡罩壁面温度的贡献就不明显了,而且此时引射流量比对遮挡罩壁面温度的影响也不太显著.

3　红外特性测试

在燃烧实验台架上对红外抑制器大模型进行红外辐射特性的测试,采用航空煤油燃烧生成高温烧气,燃气中的主要辐射成份为 H_2O 和 CO_2. 用红外光谱辐射计和响应波段为 3.63 ~ 4.84μm 的积分辐射强度计进行红外辐射亮度和辐射强度的测试. 为了评价红外抑制的抑制层次和效果,设计了一个排气截面积和波瓣喷管(不含中心锥体)相等、几何形状与弯曲混合管相似的简单排气管. 同时对红外抑制器分别采取不加遮挡罩、加遮挡罩、对遮挡罩再遮挡等方式进行测试. 实验条件:主流流量为 1.0kg/s,总温为 600℃,总压为 112 060Pa,环境温度 32℃,遮挡罩间距 30mm.

测得的主要参数为:引射流量比为 1.8,混合管出口气流最高温度 222℃,平均排气温度约 150℃,混合管壁面最高温度 180℃,遮挡罩壁面最高温度 40℃. 无抑制排气管的出口气流最高温度 554℃,平均排气温度约 400℃,混合管壁面最高温度 343℃.

图 5 为波瓣喷管红外抑制器和简单排气管的排气尾焰的光谱辐射照度,可见:两者的光谱分布具有很强的相似性,峰值辐射波长为 4.38μm,这主要是二氧化碳的波段辐射;但是峰值辐射照度的数值却差一个数量级.

图 6 为 3 ~ 5μm 波段相对辐射强度随方位角的分布,图中,以简单排气管的最大辐射强度作为基准,椭圆形排气口长轴方向为 0°方位角. 比较发现:

(1) 对无抑制简单排气管,尾焰辐射只占其总体辐射的 20% 左右;

(2) 对于未加遮挡的红外抑制器,尽管暴露的面积和排气尾焰的体积比无抑制简单排气管要高几倍,但由于温度大大降低,其红外辐射强度可以降低约 85%;这可以看作是引射冷气混合对总体红外辐射抑制的贡献;

(3) 对于加遮挡的红外抑制器,由于外露壁面温度大幅降低,相对无抑制简单排气管红外辐射强度可以降低 97%,比未加遮挡的红外抑制器又有约 10% 的衰减;这可以看作是隔热遮挡对总体红外辐射抑制的贡献;

(4) 如果再对遮挡罩进行再遮挡,使壁面辐射的影响消除,则红外抑制器的尾焰辐射强度公变无抑制简单排气管总体辐射强度的 1 ~ 2% 左右,与无抑制简单排气管的尾焰辐射相比,红外辐射强度下降了 97%.

由此可以分析出红外抑制器引射混合和隔热遮挡的作用层次:引射混合对总体红外辐射强度抑制

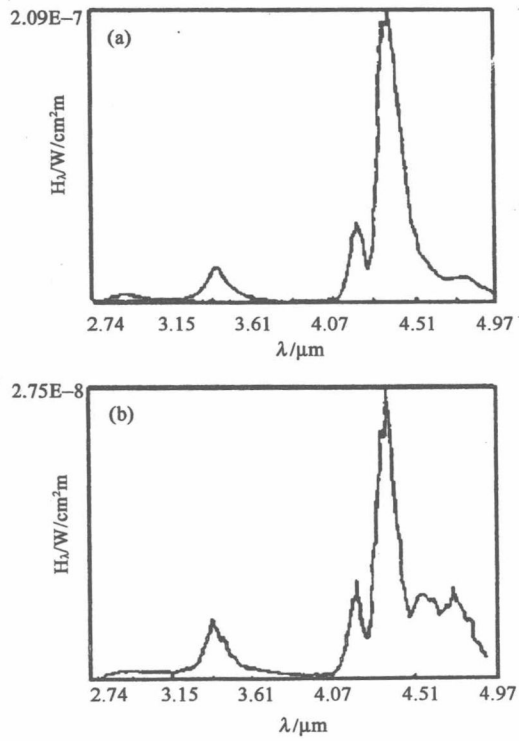

图 5　排气尾焰的光谱辐射照度
(a) 简单排气管　(b) 红外抑制器
Fig. 5　Exhaust plume irradiance
(a) simple exhaust duct　(b) IR suppressor

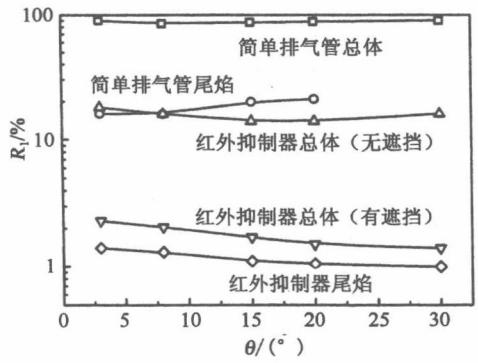

图6 相对辐射强度随方位角的分布

Fig. 6 Distribution of relative radiance intensity vs azimuthal angle

约85%；在此基础上进行隔热遮挡可以再抑制10%左右.

图7为加装遮挡罩时3～5μm和8～14μm 2个波段内的红外抑制器辐射亮度比较. 可以看出，红外抑制器尽管可把暴露热部件和排气尾焰在3～5μm波段内的红外辐射亮度降到0.15～0.29×10^{-1} W/cm^2·Sr，但是同样的目标在8～14μm波段内的红外辐射亮度仍为4.5～4.9×10^{-3} W/cm^2·Sr这样大的数值，几乎经3～5μm波段的数值大20至25倍. 由此可见，对于8～14μm波段内的红外辐射，尽管遮挡罩的最高温度降至仅比环境温度高8℃，但红外辐射仍然较强，还需与降低目标辐射率的措施相结合.

4 大小模型对比

为了分析缩比模型红外特性测试结果的可推广性，寻求不同尺度模式的红外辐射相似关系，设计了2种几何相似、几何相似比例为2的红外抑制器模型. 在对比实验中，大小模型的主流流量控制在4：1，采用相同比例的油气比，从而保证主流的速度相等而表征流动相似的雷诺数不同，主流的总温、总压和成份基本相同. 抑制器未采用遮挡罩.

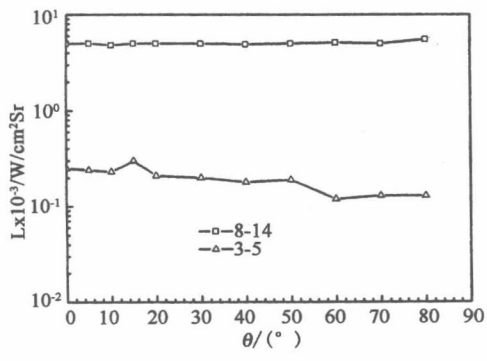

图7 辐射亮度随方位角的分布

Fig. 7 Distribution of irradiance vs azimuthal angle

实验测试得出：2种实验模型得到的引射流量比基本相同，二者相差仅6%以内；混合管椭圆形出口截面上的温度和壁面温度分布也基本相同，图8为椭圆形出口截面上沿长轴方向的温度分布情况；混合管壁面温度分布也相似，且在对应的空间位置上数值基本相等，最大温度相差4℃.

2个不同尺寸实验模型在3～5μm波段的红外辐射亮度比较见图9. 可以发现，2个实验模型的红外辐射亮度无论在数值上，还是在分布上基本一致. 表明在保持两个模型的主流速度、温度和压力均相同的条件下，由于引射流量比、混合流出口的速度和温度分布型面相似且在对应的空间位置上数值基本相等，以及混合管壁面温度分布也相似且在对应的空间位置上数值基本相等，这些因素使得表征单位面积上辐射强度的红外物理量—辐射亮度与模型尺度的相关性几乎可以不考虑. 同时，由于此时未采用遮挡罩，大模型的红外辐射亮度比采用遮挡罩时

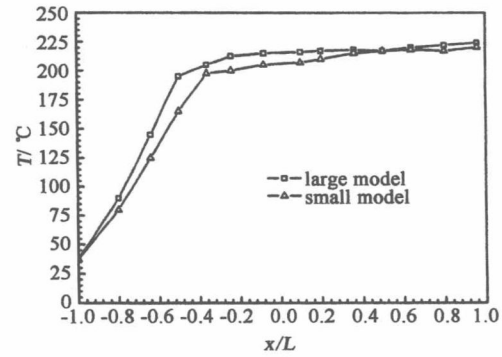

图8 椭圆形出口长轴上气流温度

Fig. 8 Mixing flow temperature distribution in the long axis of ellipse exhaust exit

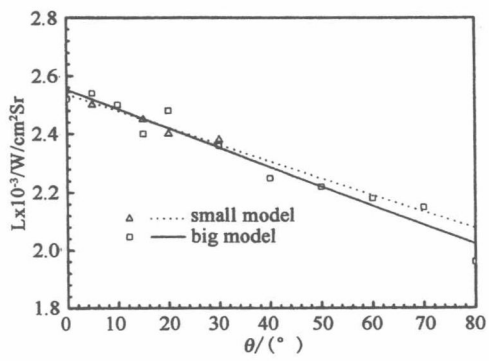

图9 辐射亮度随方位角的分布

Fig. 9 Distribution of irradiance vs azimuthal angle

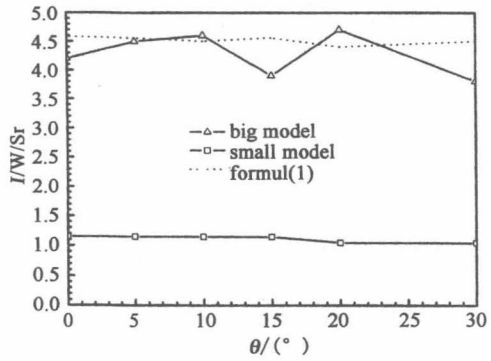

图 10　辐射强度随方位角的分布
Fig. 10　Distribution of radiation intensity vs azimuthal angle

(图 7)高出一个数量级.

图 10 为大小模型红外辐射强度的比较,图中虚线为将小模型试验数据按照式(1)

$$I_2/I_1 = s^2. \tag{1}$$

外推得到的结果. 式中 s 为几何模化比.

实验数据表明,大模型的红外辐射强度与小模型红外辐射强度之间的关系基本上遵守式(1),即在在保持 2 个模型的主流速度、温度和压力均相同的条件下,红外辐射强度基本上与模型的几何模化比平方成正比.

4　结语

本文在小型低速热喷流实验装置上对直升机排气系统红外抑制器进行了一系列的模型试验研究,结果表明:

(1) 引射冷气掺混具有降低排气温度和混合管壁面温度的双重作用,其降温效果在大引射流量比下非常显著. 因此,在红外抑制器设计中,应尽可能地寻求高引射流量比的结构设计方案.

(2) 当遮挡间距大于 20mm,遮挡隔热可以使遮挡罩壁温接近于环境温度. 当遮挡间距大于 30mm 时,再增大遮挡间距对降低遮挡罩壁面温度的贡献就非常微弱了,而且此时引射流量比对遮挡罩壁面温度的影响也不太显著.

(3) 排气尾焰的光谱辐射分布具有很强的相似性,峰值辐射波长为 4.38μm. 采取红外抑制器的排气尾焰峰值辐射照度比未抑制排气降低一个数量级.

(4) 引射混合对目标总体红外辐射强度抑制约 85%;在此基础上进行隔热遮挡可以再抑制 10% 左右.

(5) 在保持主流速度、温度和压力均相同的条件下,不同缩比模型的辐射亮度基本相当;红外辐射强度基本上与模型的几何模化比平方成正比.

REFERENCES

[1] Francois T. Internal aerodynamics of infrared suppressors for helicopter engines [C]. 40th Annual National Forum of the American Helicopter Society, 1984:1—14.

[2] Power G D, McClure M D, Vinh D. Advanced IR suppressor design using a combined CFD/test approach [R]. AIAA Paper, 94-3215,1994.

[3] ZHANG Jing-Zhou, LI Li-Guo, GAO Chao, *et al*. An experimental study on a lobed nozzle of an infrared suppression system [J]. *Journal of Aerospace Power* (张靖周,李立国,高潮,等. 波瓣喷管红外抑制系统的实验研究,**航空动力学报**),1997,**12**(2):212—214.

[4] Presz W M, Gousy R G, Morin B L. Forced mixer lobes in ejector designs [R]. AIAA Paper 86—1614,1986.

[5] Presz W M, Morin B L, Blinn R F. Short efficient ejector systems [R]. AIAA Paper 1987,87—1837.

[6] Liu Y H. Experimental and numerical investigation of circularly lobed nozzle with/without central plug [J]. *International Journal of Heat and Mass Transfer*, 2002,**45**(13): 2577—2585.

[7] Zhang Jing-Zhou, Xie Zhi-Rong. Three-dimensional computational study for flow fields within fored lobe mixer [R]. ISABE-2003-1104,2003.

[8] Birk A M, Vandam D. Infrared signature suppression for marine gas turbine; comparison of sea trail and model test result for the DRES IRSS system [J]. *ASMA Journal of Engineering for Gas Turbines and Power*, 1994,**116**(1):75—81.

[9] DU Zhao-Hui, ZHONG Fang-Yuan, ZHAO Yan. Effecct of scale factor on infrared radiation characteristics of marine exnaust system with infrared signature suppression device and its correction [J]. *J. Infrared Millim. Waves* (杜朝辉,钟芳源,赵岩. 模化比对船用排气红外抑制装置红外辐射特性的影响及修正. **红外与毫米波学报**),2001,**20**(6):437—441.

Computation and Validation of Parameter Effects on Lobed Mixer-Ejector Performances

ZHANG Jing-zhou, SHAN Yong, LI Li-guo
(*College of Energy and Power Engineering, Nanjing University of Aeronautics and Astronautics, Nanjing 210016, China*)

Abstract: Three-dimensional numerical computation of the flow fields and pumping performances for the lobed mixer-ejector are conducted using full Navier-Stokes equations. In the computation, the inlet of the primary flow uses the mass flowrate boundary condition. The inlet of the second flow and the outlet of the mixing flow use the pressure boundary condition. Compared with the relative experimental results, it is shown that the present calculation is reasonable. And a series of numerical studies is performed to obtain the effects of area ratio and length-to-diameter ratio of mixing duct on pumping coefficient and thermal mixing efficiency of a lobed mixer-ejector.

Key words: lobed nozzle; ejector; mixer; numerical computation

波瓣引射-混合器特性参数影响的数值研究和验证. 张靖周,单勇,李立国. 中国航空学报(英文版), 2005, 18(3): 193-198.

摘 要:运用不可压缩流动 Navier-Stokes 方程,对波瓣喷管引射-混合器的流场和引射特性进行了三维数值研究。在计算过程中,主流进口采用质量流量边界条件,二次流进口和混合流出口采用压力边界条件,均设置为环境大气压力。与相关的实验结果对比表明本文的计算方法可以有效地预测引射流量比和混合流场。针对混合管的结构参数开展了系列研究,获得了混合管截面比和长径比对于引射系数和热混合效率的影响趋势。

关键词:波瓣喷管;引射器;混合器;数值计算

文章编号:1000-9361(2005)03-0193-06 中图分类号:V231.1;V231.2 文献标识码:A

The mixer-ejector is an efficient fluid dynamic device consisting of a high velocity primary jet issuing from a nozzle into a mixing duct that is open at both ends. When the primary jet mixes out to fill the larger area cross-section of the mixing duct, the turbulent shear layer entrains a secondary flow. As a result of this mechanism, the ejector-mixers are widely used in aero-engine exhaust system for jet noise reduction, thrust augmentation, infrared radiation, Suppression and so on[1-3]. Mixer-ejector performances are typically expressed as the ratio of the secondary to primary mass flow rate Φ and the mixing efficiency or mixing uniformity.

A relatively large number of experimental and analytical studies, which capture the fundamental aerodynamic phenomena of the lobed mixer-ejector nozzle, have been performed[4-11]. The mixer-ejector nozzles are designed to entrain large amounts of secondary flow through an array of lobed chutes with convoluted trailing edge that are deployed into the primary stream. These lobed chutes alternating misalignment cause streamwise vortices which rapidly mix the primary and secondary flow together. The rapid internal mixing of the two streams lowers the static pressure at the nozzle exit and results in pumping capacity augmentation.

However, the knowledge about the effects of design parameters and geometric configuration on the mixer-ejector performances are not enough by now. Furthermore, the attempt to seek a reasonable method for predicting the pumping capacity of the mixer-ejector is also important. For this reason, analytical design tool is a key aspect to the successful design process, which not only saves ex-

Received date: 2004-03-26; Revision received date: 2005-03-30
Foundation item: Aeronautical Science Foundation of China

pensive and time-consuming by test compared to CFD analysis, but also is helpful to obtain detailed insight of the flow physics in the mixer-ejector nozzle solely from test data.

To the authors' s knowledge, the numerical simulation of mixer-ejector pumping capacity is a challenging problem for the reason that the secondary flow is driven solely by the primary entrainment. In the early time, the pumping capacity prediction is based on 1-D mixing analysis[12] in which conservation of mass flow rate, momentum, and energy are enforced. This method may predict the ideal limit for giving no consideration on the effects of the wall friction and non-uniformity of the mixing process. Zhang and Shan[13] made an improvement by using 1-D ejector pumping relationship and full Navier-Stokes equations. Firstly, the ideal pumping coefficient was determined based on the 1-D ejector pumping relationship. Then the coefficients in the 1-D ejector pumping relationship were corrected according to the velocity distribution and wall friction resulting from the calculation of Navier-Stokes equations. So the final pumping coefficient was obtained by repeating the above process until the residual was satisfied. From the comparison between the computation results and experimental data, it was concluded that this method is reasonable in predicting the mixer-ejector pumping capacity.

The objective of this paper is to present a numerical computation and validation of pumping and mixing characteristics for lobed mixer-ejector based on Fluent-CFD software with the use of full Navier-Stokes equations and two-equation turbulence model. Especially it focuses on the research of boundary condition assignments at the inlet and outlet plane, to seek the reasonable treatment for determining the mixer-ejector pumping capacity. And a series of mixing duct parameters are varied, such as the diameter and length, to obtain better insight into the influences of mixing duct parameters on lobed mixer-ejector performance and compared with experimental data.

1 Experimental Description

The mixer-ejector test facility is shown schematically in Fig.1. The primary flow is high pressure cold air supplied by the air compressor. It flows through a duct with diameter 80 mm. After being heated by the combustor, the primary stream with high velocity and temperature enters the lobed nozzle. The lobed nozzle has 12 lobes distributed uniformly in circumferential direction (Fig.2). The lobe height $h = 28$ mm, lobe width $b = 7.2$ mm with the sides being parallel to each other, lobe length $l_b = 80$ mm with the expend angle of the lobe is 20°. The secondary stream is entrained to a larger chamber through two ducts having standard bell-mouth inlet located up and down of the chamber. The two flows mix in the mixing duct with constant area section and then exhaust to the ambient.

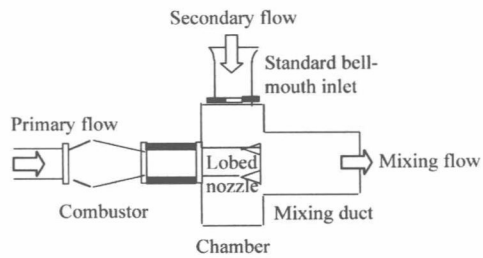

Fig.1 Schematic of test facility

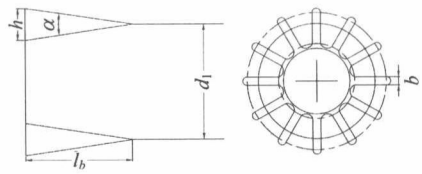

Fig.2 Simplified mixer-ejector configuration

The primary mass flowrate m_p is measured by a standard orifice plate flowmeter located in the primary air supply pipe upstream of the combustor. The primary total pressure and temperature are measured by pressure and temperature probes respectively. The secondary mass flowrate m_s is determined by static pressure in the standard bell-mouth inlet.

The temperatures of mixing flow at mixing duct exit are measured by temperature probes. And the static pressure holes on the mixing duct wall are aligned in two lines corresponding to lobe peak and

lobe trough in circumference respectively.

In the present work, the parameters of lobed nozzle are constant, a series mixing duct parameters are varied by changing the diameter and length of the mixing duct.

2 Numerical Procedure

2.1 Computation region

As the experimental model is axial-symmetric, only half of the physical model is chosen as computational region(Fig.3). The unstructure grids are used in the present computation and refine grids are placed near the solid wall. From CFD test it is appeared that 417 249 grid points are adequate for solving the mixing-related features of the flow field, as well as determining the pumping characteristics of the mixer-ejector.

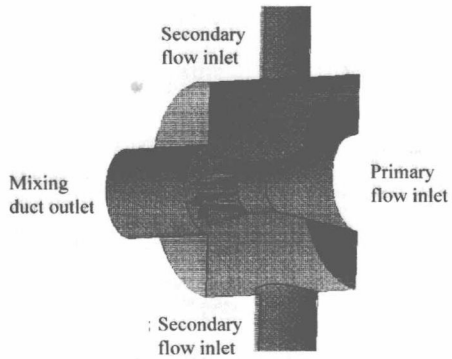

Fig.3 Schematic of computation model

2.2 Boundary conditions

The governing equation in general form is

$$\frac{\partial}{\partial x}(\rho u\phi)+\frac{1}{r}\frac{\partial}{\partial r}(r\rho v\phi)+\frac{1}{r}\frac{\partial}{\partial \theta}(\rho w\phi)=\frac{\partial}{\partial x}\left(\Gamma\frac{\partial \phi}{\partial x}\right)+\frac{1}{r}\frac{\partial}{\partial r}\left(\Gamma r\frac{\partial \phi}{\partial r}\right)+\frac{1}{r}\frac{\partial}{\partial \theta}\left(\frac{\Gamma}{r}\frac{\partial \phi}{\partial \theta}\right)+S \tag{1}$$

The turbulent viscosity is defined as

$$\eta_t = c_\mu f_\mu \rho k^2/\varepsilon \tag{2}$$

The coefficients in the above equations are determined by RNG k-ε model[14].

The boundary conditions required for the mixer-ejector calculation are the mass flowrate and temperature of the primary, ambient pressure and temperature.

Flowrate boundary type is used at the primary flow inlet, with the mass flux 0.108 kg/s and temperature 620 K.

Pressure boundary types are used at the secondary flow inlet and mixing flow outlet, with pressure 101 325 Pa and temperature 300 K. The derivations of all the variables along streamwise direction are set as zero.

The velocities at the wall are set as zero and the adiabatic wall condition is applied to the energy equation. The wall law is used to treat k and ε near the wall.

Symmetry boundary condition is employed at the central plane.

The convergence degree for velocities, k and ε is chosen as 10^{-4}, for temperature is 10^{-6}.

3 Results and Discussion

3.1 Comparison of computation and experiment

A comparison of the calculated and measured temperature radial distributions[10] at the mixing duct exit for the case of the area ratio $\lambda=3.3$ (λ is defined as the area ration of mixing duct area to nozzle area) and the length-to-diameter ratio $L/D=1$ is shown in Fig.4. The temperatures are the average values in radial direction among the fan section from lobe peak to lobe trough. This comparison demonstrates reasonably good agreement between the computed and measured results, which indicates that the computational procedure in the present work is reliable to simulate the mixing flow fields.

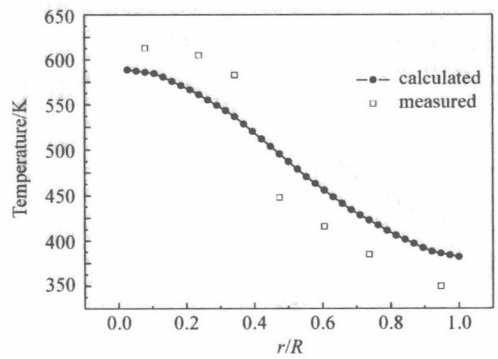

Fig.4 Comparison of calculated and measured temperature radial distributions

The comparison of the measured and calculated mixing duct static pressure distributions in the case of $\lambda=3.3$ and $L/D=1$ is shown in Fig.5.

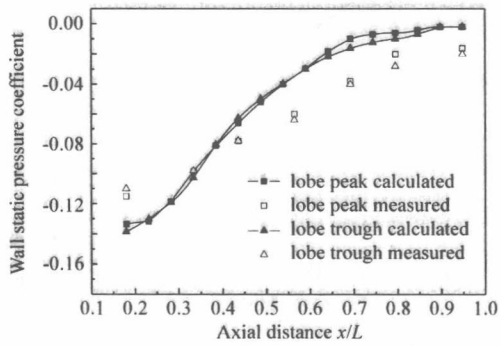

Fig.5 Static pressure distributions on mixing duct

The pressure coefficient define as

$$C_P = (p - p_{atm})/(0.5\rho u_p^2) \quad (3)$$

It is found that there are good agreements between the measured and calculated values in the lobe peak or trough section. The static pressure near the nozzle exit is lower and then increases gradually to ambient pressure.

Fig.6 shows the comparison of the calculated and measured pumping ratio for different area ratios of mixing duct.

$$\Phi = m_s/m_p \quad (4)$$

here m_s is the secondary massflow and m_p is the main massflow.

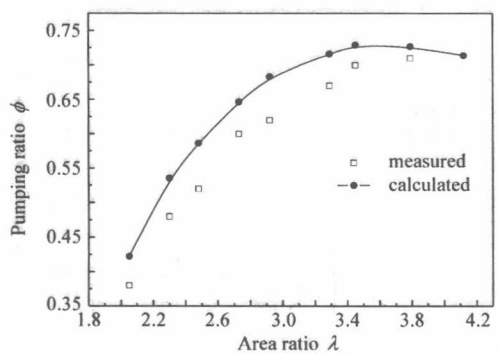

Fig.6 The relationship of pumping ratio *vs* area ratio

From the comparison, it is seen that the calculated values are some greater than the corresponding experimental values and the tendency for Φ-λ is the same. The maximum relative disagreement is about 20% in the little area ratios. It seems that, the disagreement between the calculated and measured values is acceptable and realistic. Firstly, the computational model is "ideal" while the "sophisticated" factor, including the smooth of solid wall, conjugate between the test section and manufacture accuracy of the real experimental model, are not considered. Secondly, the difference between the calculated mixing flow fields and real mixing flow fields also contributes the disagreement between the calculated and measured pumping ratio values. Generally, the present computational procedure for predicting the pumping ratio of mixer-ejector is satisfactory.

3.2 Parameter effects on performances

Fig.7 shows the calculated temperature radial distributions at the mixing duct exit for the case of the area ratio 3.3 and the length-to-diameter ratio 0.8-2.5. As the length-to-diameter ratio increases with the area ratio being constant, the maximum temperature at the centerline of the mixing duct decreases and the minimum temperature near the wall increases. The uniformity of the temperature radial distribution also reflects the mixing efficiency of the mixer-ejector.

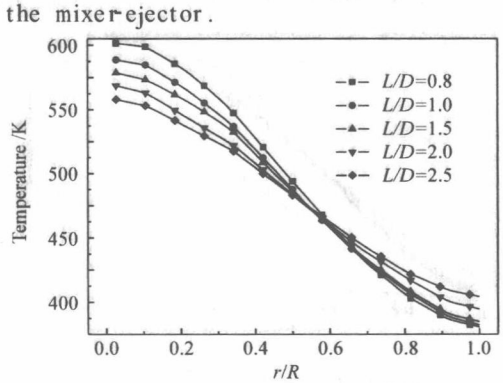

Fig.7 Temperature radial distributions at mixing duct exit (varying length)

In order to evaluate the thermal mixing state quantitatively, the thermal mixing efficiency is defined as

$$\eta = \frac{\int T^{0.5}\,\mathrm{d}\,m - T_P^{0.5} m_p - T_s^{0.5} m_s}{T_{mix}^{0.5}(m_p + m_s) - T_P^{0.5} m_p - T_s^{0.5} m_s} \quad (5)$$

where T is the static temperature and T_{mix} is the temperature of fully mixed flow.

The thermal mixing efficiencies along the mixing length in the case of $\lambda = 3.3$ and $L/D = 1$ are shown in Fig.8. As x/L increases, the thermal mixing efficiency increases rapidly, showing that the thermal mixing efficiency is increasing. It is obvious that the streamwise vortices have an im-

portant role on enhancing rapidly mixing the primary and secondary flow together and reducing the core temperature of primary flow.

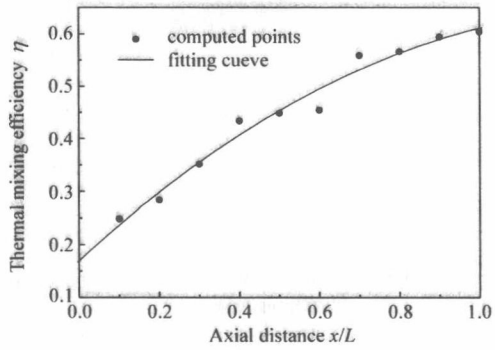

Fig.8 Thermal mixing efficiency *vs* axial distance

Fig.9 shows the variation of the thermal mixing efficiencies at the mixing duct exit for different mixing duct lengths and area ratios, respectively. It is shown from Fig.9(a) that the thermal mixing efficiency increases along with the increased length of the mixing duct for a giving value of mixing duct area ratio, which indicates that the increase of mixing duct length have a benefit to enhance the thermal mixing efficiency. This mixing characteristic is continent with the pumping feature, and for a giving mixing duct area ratio, the improvement of mixing efficiency is corresponding to the enhancement of pumping capacity.

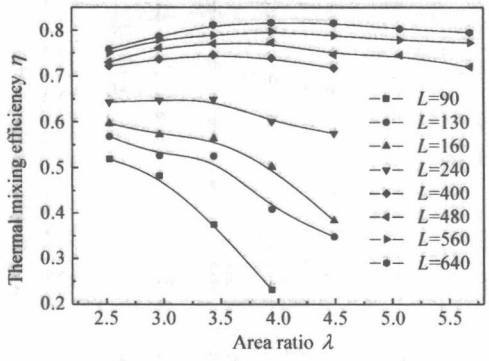

(a) Thermal mixing efficiency *vs* area ratio

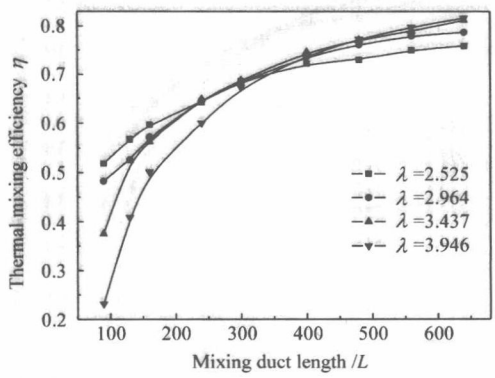

(b) Thermal mixing efficiency *vs* mixing duct length

Fig.9 Thermal mixing efficiency at the mixing duct exit

For a giving value of mixing duct length, the relationship of thermal mixing efficiency vs mixing duct area ratio is more complicated than the former Fig.9(b). On the cases of short mixing duct length, the increase of area ratio (*i.e.*, the increase of the mixing duct diameter) induces the reduction of the thermal mixing efficiency. On the cases of long mixing duct length, the increase of area ratio causes the up-down process of the thermal mixing efficiency. As known that the pumping capacity is associated with both mixing efficiency and secondary flow area, so the mixing characteristic is not continent with the pumping feature in the case of varying mixing duct area ratio.

A series of computations for determining the effects of area ratio and length-to-diameter ratio on the pumping capacity are shown in Fig.10. It is seen that there is a peak pumping ratio value to correspond one λ for a giving mixing duct length and the λ corresponding to the peak pumping ratio increases as the mixing duct length increases. This feature is continent to the research by Skebe *et al*[15], which indicates that there is an optimum performance design for the particular mixer-ejector system.

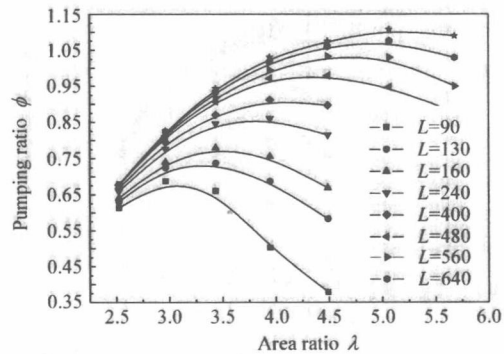

Fig.10 Effects of mixing duct parameter on pumping ratio

4 Conclusions

Numerical computation and validation of the flow fields and pumping performances for the lobed mixer-ejector are conducted using full Navier-

Stokes equations. In the computation, the inlet of the primary flow uses the velocity boundary condition, and the inlet of the second flow and the outlet of the mixing flow use the pressure boundary condition. Compared with the relative experimental results, it is shown that the present calculation is satisfactory for predicting pumping capacity of mixer-ejector.

The mixer-ejector performances with variation of the area ratio and length-to-diameter ratio of the mixing duct are also demonstrated.

References

[1] Presz W M, Reynolds G, McCormick D C. Thrust augment using mixer-ejector-diffuser systems[R]. AIAA Paper 94-0020, 1994.

[2] Presz W M. Mixer/ejector noise suppressors[R]. AIAA Paper 91-2243, 1991.

[3] 张靖周,李立国,高潮,等.波瓣喷管红外抑制系统的实验研究[J].航空动力学报,1997,12(2):212-214.
Zhang J Z, Li L G, Gao C, *et al*. Experimental study on lobed nozzle IR suppression[J]. Journal of Aero Power, 1997, 12(2): 212-214.(in Chinese)

[4] Presz W M, Gousy R G, Morin B L. Forced mixer lobes in ejector designs[R]. AIAA Paper 86-1614, 1986.

[5] DeBonis J R. Full navier-stokes analysis of a two-dimensional mixer/ejector nozzle for noise suppression[R]. AIAA Paper 92-3570, 1992.

[6] Malecki R, Lord W. Navier-stokes analysis of a lobed mixer and nozzle[R]. AIAA Paper 90-0453, 1990.

[7] Koutmos P, McGuirk J J. CFD predictions of lobed mixer performance. Computer Methods in Applied Mechanics and Engineering[J]. 1995, 122: 131-144.

[8] Salman H, McGnirk J J, Page G J. A numerical study of vortex interactions in lobed mixer flow fields[R]. AIAA Paper 99-3409, 1999.

[9] Ooba Y, Kodama H, Nakamura Y. Large eddy simulation analysis of a 18-lobe convoluted mixer nozzle[R]. AIAA Paper 2002-0717, 2002.

[10] Liu Y H. Experimental and numerical investigation of circularly lobed nozzle with/without central plug[J]. International Journal of Heat and Mass Transfer, 2002, 45: 2577-2585.

[11] Zhang J Z, Xie Z R. Three-dimensional computational study for flow fields within forced lobe mixer[R]. ISABE Paper 2003-1104, 2003.

[12] Presz W M, Morin B L, Blinn R F. Short efficient ejector systems[R]. AIAA Paper 87-1837, 1987.

[13] 张靖周,单勇.二维引射—混合器流场的数值研究与验证[J].航空动力学报,2002,17(5):524-527.
Zhang J Z, Shan Y. Numerical study and examination of 2D mixer-ejector[J]. Journal of Aero Power, 2002, 17(5): 524-527.(in Chinese)

[14] Yakhot V, Smith L M. The renormalization group, the ε expansion and derivation of turbulence model[J]. Journal of Scientific Computing, 1972, 7(1): 35-62.

[15] Skebe S A, McCormick D C, Presz W M. Parameter effects on mixer-ejector pumping performance[R]. AIAA Paper 88-0188, 1988.

Biographies:

ZHANG Jing-zhou Born in 1964, Professor, he received B.S. from Tsinghua University in 1986 and M.S. from Southeast University in 1989 and doctoral degree from Nanjing University of Aeronautics and Astronautics in 1992 respectively. He has done a lot of researches on mixer-ejector and enhanced heat transfer, and published several scientific papers in various periodicals. E-mail: zhangjz@nuaa.edu.cn

SHAN Yong Born in 1978, Ph.D student, he received B.S. and M.S. from Nanjing University of Aeronautics and Astronautics. Now he is working for his doctoral degree. His research interests are infrared stealth. Tel: 025-84892200-2523. E-mail: nuaasy@tom.com

LI Li-guo Born in 1935, Professor, he received B.S. from Huazhong University in 1952 and then became a teacher in Nanjing University of Aeronautics and Astronautics. He has done a lot of researches on mixer-ejector and enhanced heat transfer, and published many scientific papers in various periodicals.